Sustainable Development Research; Vol. 5, No. 1; 2023
ISSN 2690-9898 E-ISSN 2690-9901
https://doi.org/10.30560/sdr.v5n1p44

Gwal Pahari Acid: Isolation, Characterization of a New Soil Based Plant Growth Promoting Humic Acid

Sujeet Kumar Thakur[1], Krishnendu Goswami[2], Ankit Kumar[3], Saikat Bhattacharjee[2] & Sambasivan Venkat Eswaran[4]

[1] TERI School of Advanced Studies, (Plot No. 10, Vasant Kunj Institutional Area), New Delhi, India

[2] Regional Centre for Biotechnology (RCB), under the auspices of UNESCO-DBT, (NCR Biotech Science Cluster), 3rd Milestone, Faridabad-Gurgaon Expressway, Faridabad, Haryana, India

[3] Teri Deakin Nano Biotechnology Research Centre (TERI Gram, The Energy and Resources Institute, Gwal Pahari, Gurgaon – Faridabad Road, Gurgaon, Haryana, India

[4] Ex: Head (Chemistry Department) and Dean (Academics), St Stephen's College, Delhi, 110007; Amity University, Noida, Uttar Pradesh-201313, India; Adjunct Prof. (Hony.), Deakin University, Australia; Teri Deakin Nano Biotechnology Research Centre, Gwal Pahari, TERI Gram, The Energy and Resources Institute, Gurgaon Faridabad Road, Gurgaon, Haryana, India

Correspondence: Sambasivan Venkat Eswaran, Ex-Head (Chemistry Department) and Dean (Academics), St Stephen's College, Delhi, 110007; Amity University, Noida, Uttar Pradesh-201313, India; Adjunct Prof. (Hony.), Deakin University, Australia; Teri Deakin Nano Biotechnology Research Centre, Gwal Pahari, TERI Gram, The Energy and Resources Institute, Gurgaon Faridabad Road, Gurgaon, Haryana, India. E-mail: sv.eswaran@gmail.com

Received: March 16, 2023 Accepted: May 1, 2023 Online Published: May 3, 2023

Abstract

There are many “Save the Soil” movements highlighting the degradation of the soil due to excessive use of fertilizers, ground water contamination and environmental pollution. An alternative strategy is the use of humic acids from Organic Matter (OM) in soils. Humic acids help grow better vegetables, quality fruits like (peas, potatoes, tomatoes, pomegranates, mangoes), cereals, and pulses. These create supramolecular self– assemblies capable of retaining water and not allowing loss of minerals and ions. Humic acids isolated from soil, lignite and city solid waste are emerging as attractive sources for developing value added products from them. There is much interest in exploiting the commercial aspects in the energy sector of the economy as these new technologies could help in cleaning the environment as well.

In this paper, the isolation of a new humic acid from the soil of Gwal Pahari, Gurgaon, Haryana, India is described. This water soluble, Ninhydrin positive Gwal Pahari Acid (GPA) contains thirteen chiral centers and contains both partly rigid and dynamic systems capable of exhibiting pseudo rotation. The proposed structure of this new humic acid is based on spectroscopic studies (e.g. FT-IR, UV-visible spectroscopy), detailed mass spectrometry, and very challenging ^{1}H- NMR and 2D-NMR studies. Ion leakage studies on *Arabidopsis thaliana* have shown that the new compound provides protection to the plant, and greenhouse studies demonstrate that Gwal Pahari Acid brings about substantial growth in the tomato plant.

Keywords: Humic acids, Ion leakage, *Arabidopsis thaliana*, Tomato, NMR

1. Introduction

There is much interest in exploiting the commercial aspects of humic acids which serve as growth promotants in plants. Their mode of action is through chelating cations and their water retention ability (de Melo et al. 2016; Eladia et al. 2005). Humic and fulvic acids are known from soils and sediments from different parts of the world (El-Metwally et al. 2014; Beckely, 1921). Two structures assigned to these are shown below as examples in Figure 1:

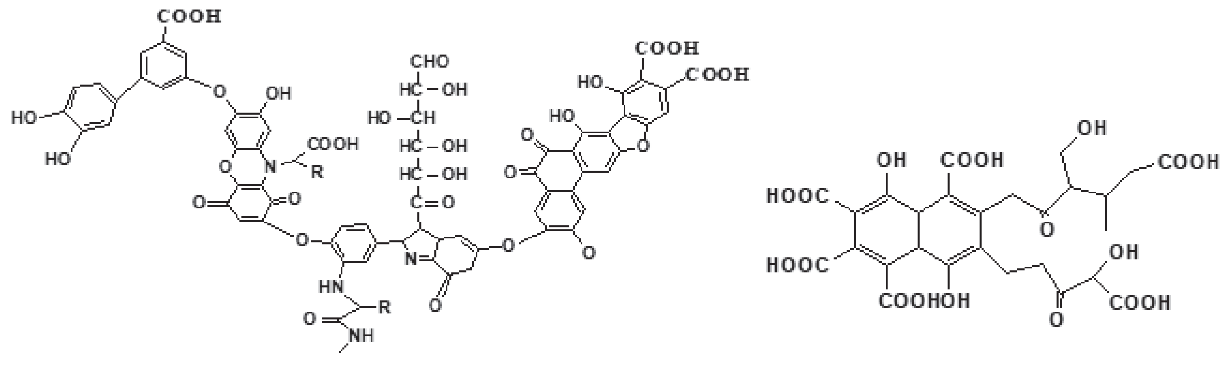

(a)Humic Acid Molecule (b) Fulvic Acid Molecule

Figure 1. Examples of humic substances

Among the areas already captured by these substances for large scale use include important areas of agriculture and horticulture. These compounds possess multiple functionalities and through intelligent use could lead to newer areas of industrial exploitation. Through newer and innovative technological developments, humic acids are now being considered important for the energy sector of the economy as well. Based on these Dye Sensitized Solar Cells (DSSCs) have been described (Vekariya et al. 2016). Most recent reports point to the fact that unlike what has been believed in the past, many of such molecules are relatively simple small molecules. Most papers show spectra but refrain from putting down a precise chemical structure. This is because these form large assemblies and form supramolecular structures (Figure 2), whose formation is critically dependent on pH (Piccolo, 2002).

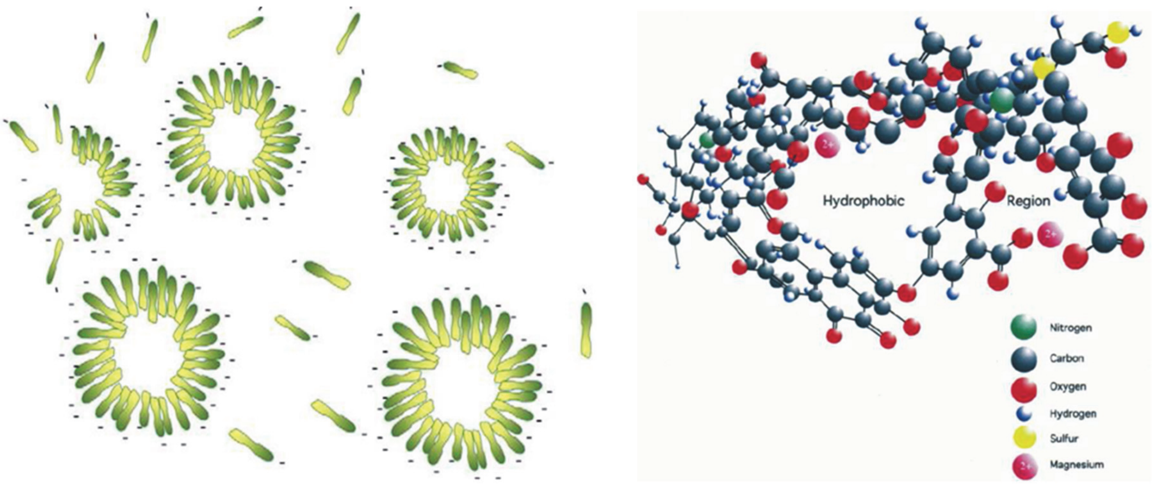

(a) (b)

Figure 2. (a)Picture of micelle formation of a Humic Substance

(b)Model of a supramolecular structure of a Humic acid

Among the many techniques like FT-IR (Tatzber et al. 2007), UV-Visible spectroscopy (Fasurova, 2010), Scanning Electron Microscopy (Tan, 1985), Mass spectrometry (Stenson et al. 2002; Shinozuka, 2004), ^{1}H-NMR, ^{13}C-NMR spectroscopy (Abakumov, 2015; Giovanelaa et al. 2010) are commonly used. More recent studies use CP-MAS-SS NMR (Al-Faiyz, 2017), which pick up and identify broad peaks for the aliphatic/ alicyclic and aromatic regions. Previous studies on humic acids also show the plant growth promoter activity and enhancement of yield in Potatoes.

Humic acids have tremendous effect on healthy colonic microbiome and potentially interesting substances for the development of drugs that control the innate colonic microbiome (Mirza et al. 2011; Swidsinski et al. 2017). Humic Acid (HA) has also been evaluated for the oral drug delivery of carbamazepine and its pharmacodynamic – responses during the delivery process (Gajdosová et al. 2001). A question has been raised, as to whether humic acids are present in Antarctica (Gajdošová et al. 2003). Ion leakage assay (Hatsugai, 2018) is a convenient way to measure the cell membrane stability, as leakage of more ions denotes less stability of plant membrane in the plant cell, which is vital to control the water stress condition and membrane injury (De Nobili et *al.* 1990; Thurman, 1981).

In this paper, we describe the isolation of a new amino acid, a humic acid and its extraction from the soil of Gwal Pahari, Gurgaon, Haryana using the standard procedure of International Humic Substances Society, (IHSS), USA (Hendrickx, 2008). The optically active new amino acid has been investigated using spectroscopic techniques like UV-Visible, FT-IR, MALDI- MS, zeta potential, ^{1}H-NMR, and 2D–NMR. A deep purple color was obtained in the Ninhydrin test showing it to be an amino acid, which has been named as Gwal Pahari Acid (GPA).

1.1 Experimental

All the reagents and solvents were purchased from Sigma Aldrich (greater than 99.9 % purity). UV – visible spectrum was recorded in methanol at room temperature using a Perkin Elmer Lambda 35 double beam spectrophotometer. Scanning Electron Microscopy (SEM) was recorded using the SEM Zeiss EVO MA 10 in methanol solution. Initial ^{1}H-NMR studies were done in the International Centre for Genetic Engineering and Biotechnology (ICGEB, New Delhi) & Translational Health Science and Technology Institute (THSTI), Faridabad. ^{1}H-NMR, 2D-NMR, temperature dependent NMR, solid state NMR spectra were recorded using Bruker 500 MHz NMR instrument in D_2O solution in Tata Institute of Fundamental Research (TIFR), Hyderabad. Mass spectrum of this compound was recorded in (THSTI), Faridabad, and MALDI-MS spectrum was recorded in the Regional Center for Biotechnology (RCB, Faridabad) in methanol solution and GC-MS was recorded in methanol solution using Mass Hunter GC/MS Acquisition B Agilent Technologies, Inc., at IIT Delhi. FT-IR studies were performed using Bruker Tensor 27 FT-IR with Diamond ATR cell in methanol solution. Optical rotation was recorded in solution phase using circular Dichroism spectro-polarimeter specification JASCO, J-815CD spectrometer (Department of Chemistry, University of Delhi).

1.2 Bioassay for plant growth promotion properties of Gwal Pahari Acid (GPA)

The seeds of tomato (*Solanum lycopersicum*) were surface sterilized using ethanol (70%) for 1 min. and sodium hypochlorite solution (2%) mixed with Tween-20 (0.02%) for 5 min. in a 100 ml conical flask by vigorously shaking with the sterilizing reagents (Subramanian et al*.,* 2015). Following this, seeds were washed repeatedly with plenty of sterilized water (at least three times for 3-5 min.), to remove or minimize the population of seed-associated micro flora. The surface sterilized seeds were kept in Petri dishes (10-20 seeds/Petri dishes) and incubated for 48 h in a growth chamber at 25°C ± 1°C with a 16 h photoperiod and allowed to germinate. The germinated seeds with the same root length (1 mm) were selected and transferred to the pots (2 Kg) containing a mixture of sterilized soil and sand (1:1; w/w). The soil and sand were separately sterilized twice consecutively in an autoclave (121°C for 1 h). To study the preliminary analysis of impact of GPA on tomato plants, five conc. of GPA were randomly selected ranging from 100 ppm – 500 ppm for treatments. The treatment details include: T_1: Tomato seedlings treated with 100 ppm of GPA; T_2: Tomato seedlings treated with 200 ppm of GPA; T_3: Tomato seedlings treated with 300 ppm of GPA; T_4: Tomato seedlings treated with 400 ppm of GPA; T_5**:** Tomato seedlings treated with 500 ppm of GPA. The untreated tomato seedlings were treated with sterile water which served as absolute control for comparison. There were three replicates of each treatment as well as control. After the seedlings were sown, the pots were kept for 6 weeks in a Greenhouse at 25°C ± 2°C, relative humidity (RH) maintained between 50%-70% and average photoperiod of 12 h/day. The pots were kept in a randomized block design to minimize the impact of microsite location in the Greenhouse. The plants were irrigated with sterile water as and when required. For analysis, destructive sampling was carried out and the plant samples were studied for root length (RL), shoot length (SL), fresh wt. (FW) and dry wt. (DW) in terms of plant growth promotory potential of GPA. The data was analyzed using ANOVA software.

1.3 Plant Growth Conditions for Ion Leakage Assay

Arabidopsis thaliana seeds were stratified at 4°C in dark for three consecutive days. Then the seeds were washed with 30% bleach solution for surface sterilization followed by rinsed three times with sterile water. Murashige and Skoog (MS) agar media containing petri-dishes (0.5X MS, 0.5% sucrose, 1% phytoagar, pH 5.7) prepared for platting the seeds, the plates were sealed with parafilm and placed in sterile condition under the short day (12 hr dark: 12hr light) photoperiod cycle and with a constant temperature of 22°C for 7 days. Then seedlings were planted on soil. In continuous interval of 2 days, we supplemented the plant with our desired compound dissolved in water (20 Micro Mol.) for 16 days. The control sample was treated with water only.

2. Material and Methods

2.1 Isolation of "Gwal Pahari Acid"

The extraction of title compound followed the protocol of the International Humic Substances Society (IHSS). 500 gm of Gwal Pahari soil was taken in a conical flask and washed with 1% aqueous HCl solution and left for stirring overnight. The solution was then filtered and the liquid extract discarded. The residual solid thus obtained was treated with 10% aqueous sodium hydroxide (NaOH) solution and stirred overnight at room temperature maintaining the pH at 7.4. The solution was then centrifuged at 15000 rpm for 1 hour. The liquid extract was then acidified with conc. HCl up to pH 2-3. The acidic solution was subjected to liquid-liquid extraction with ethyl acetate. The ethyl acetate layer, containing the minor product was separated and sodium sulphate anhydrous added to this layer and kept in the refrigerator. This aqueous portion was allowed to evaporate in sunlight (up to 3-4 days) shown in Scheme-1.

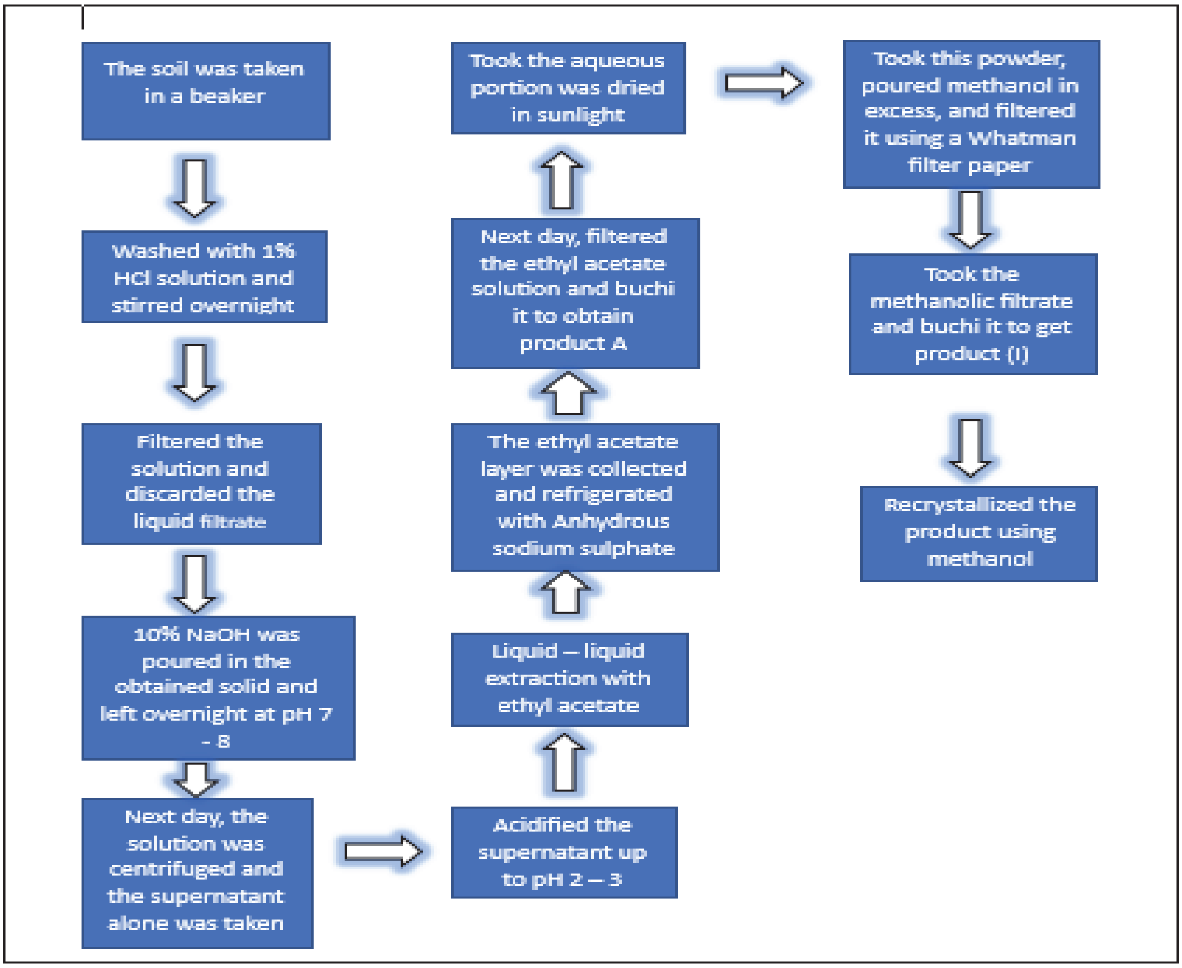

Scheme 1. Flow chart for the extraction of Gwal Pahari Acid

After complete drying we scratched out the entire portion and extracted two to three times with methanol. The solvent was evaporated using Buchi evaporator gave the product; Yield 3 g (0.6 %); Melting point, 346^{O} C.

2.2 Synthesis of Gwal Pahari Acid -Doxorubicin Conjugate

(i) Synthesis of Gwal Pahari Acid –N-Hydroxy Succinimide Conjugate:

1 g of GPA was taken in a round bottomed flask and 260 mg of DCC was mixed with 200 mg of NHS and 75 ml of dichloromethane was added. The reaction mixture was stirred overnight at room temperature. The reaction mixture was filtered the next day to remove the insoluble part and the solvent evaporated from the filtrate using a Buchi evaporator to give off white solid and dried in P_2O_5-vacuum (Yield. 432 mg).

(ii) Synthesis of GPA-Doxorubicin Conjugate:

Took 50 mg of the above GPA- NHS conjugate in a round bottomed flask with 15 ml of dichloromethane and the 92 mg Doxorubicin base was prepared using methanolic sodium bicarbonate ($NaHCO_3$) in a separate flask. A change in color from orange red to blue was observed and it was immediately subjected to Buchi evaporator to remove all the solvent. 10 ml of dichloromethane was added to solubilize all the material and the contents mixed with the GPA-NHS conjugate solution. This reaction mixture was subjected to overnight stirring at room temperature in the dark. Next day it was filtered to remove the insoluble content and subjected to Buchi evaporation. After drying over P_2O_5-vacuum, 27 mg of the dark red solid was obtained.

3. Results

The title compound, “Gwal Pahari Acid”, a new Humic acid was extracted from soil of Gwal Pahari (Figure 3), Teri Gram, Gurgaon, Haryana, India using the International Humic Substances Society (IHSS) protocol.

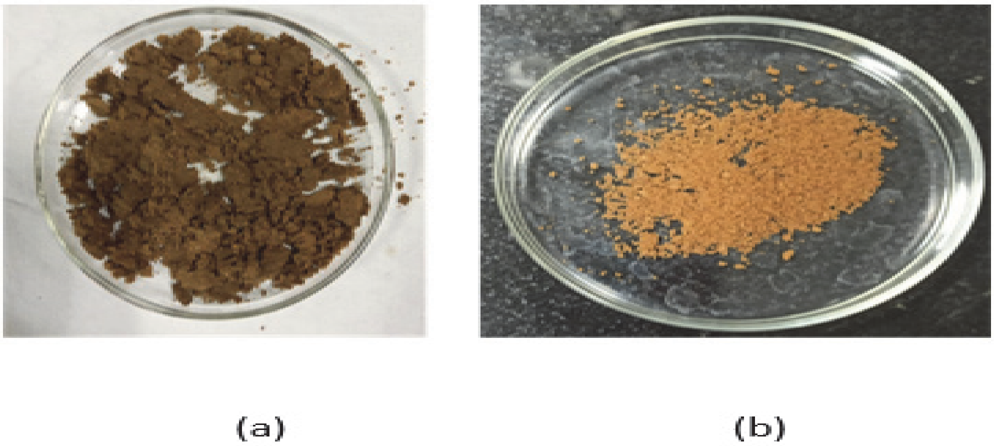

Figure 3. (a) Images of Gwal Pahari Acid (Starting materials) (b) Gwal Pahari Acid (Product)

4. Mass Spectral Studies

The mass spectral studies of the title compound were performed in methanol solution. Mass spectrum of the new compound is shown in the Figure 4.

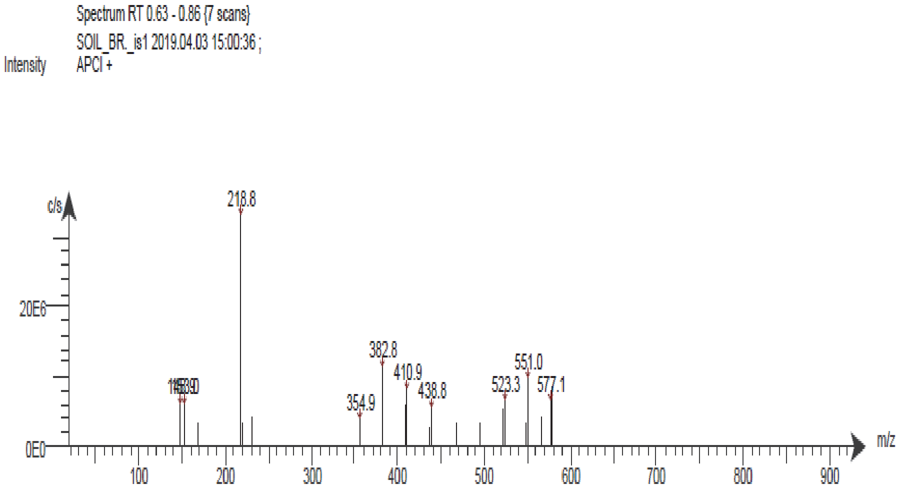

Figure 4. Mass spectrum of GPA

The spectrum showed a peak at m/z 577.1 and another peak one unit higher at namely M^+ 578.1 which readily lost a proton. Other fragment peaks were observed at m/z 551, 523.3, 438.8, 410.9, 382.8, 354.9 and the base peak was observed at m/z 218.8.

4.1 UV-Visible Spectral Studies of Gwal Pahari Acid

The UV-visible spectrum was recorded in methanolic solution and the obtained peaks at 223, 244 and 299 nm shown in Figure 5.

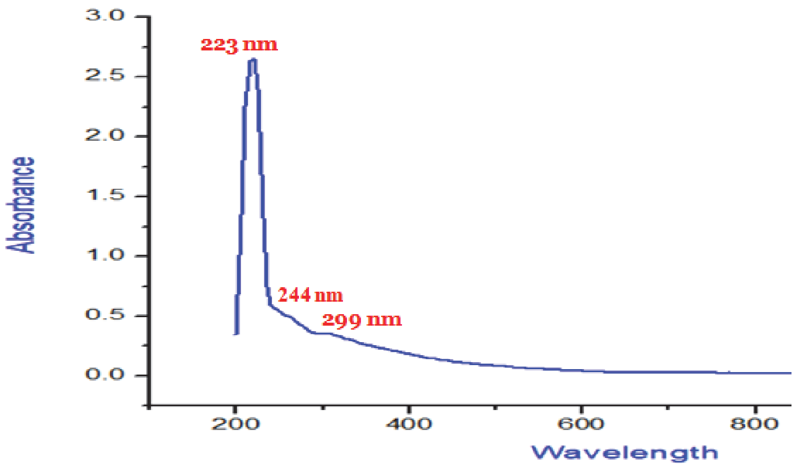

Figure 5. UV- visible spectrum of GPA

4.2 FT-IR Spectral Studies on Gwal Pahari Acid

FT-IR spectral studies of new Gwal Pahari Acid were done in methanol solution. This spectrum shows different peaks at 576, 961, 1423, 1692, 2115, 2422, 2999 and 3461 cm^{-1} (Figure 6).

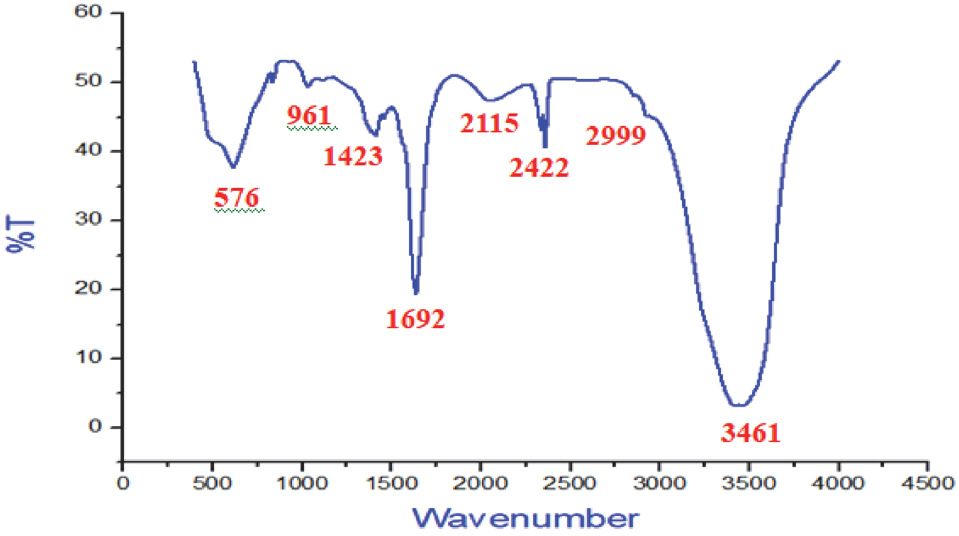

Figure 6. FT-IR spectrum of GPA

4.3 NMR spectral studies on Gwal Pahari Acid

^{1}H- NMR spectral studies:

NMR spectra were recorded in D_2O using a Bruker 500 MHz instrument. ^{1}H-NMR spectrum of GPA is shown in (Figure 7).

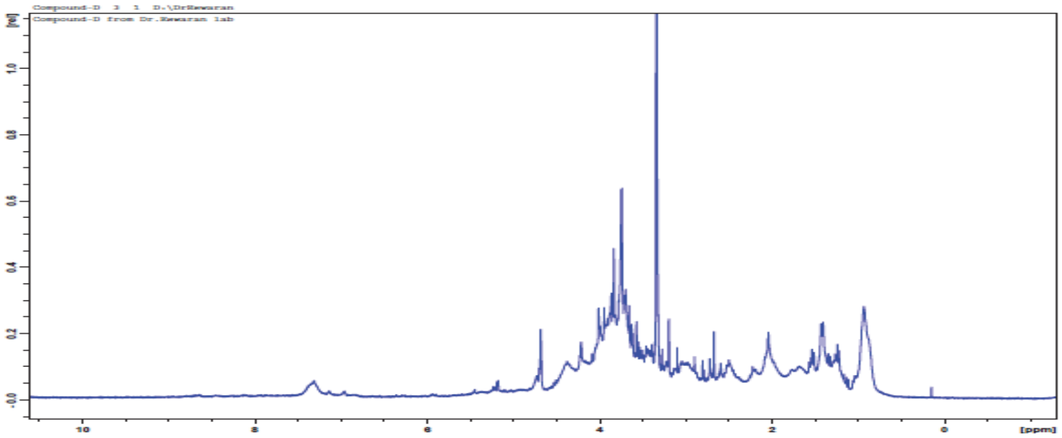

Figure 7. ^{1}H NMR spectrum of Gwal Pahari Acid

The ^{1}H-NMR spectrums clearly showed signals only in the aliphatic/ alicyclic region δ 3.33, δ 0.0 to 0.5 and δ 0.93 ppm**.**

4.4 2D-NMR spectral studies of Gwal Pahari Acid

2D-NMR spectral studies were then taken up to establish the correlations between the different substituents. The HSQC spectrum of GPA is shown in (Figure 8).

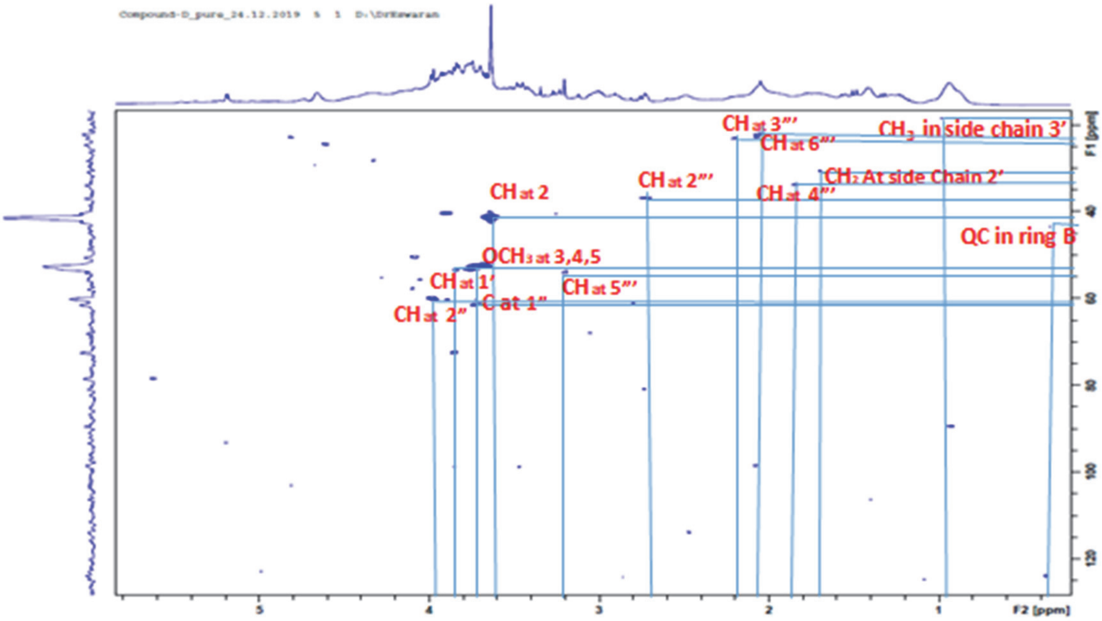

Figure 8. HSQC spectrum of Gwal Pahari Acid for δ 0-6 ppm region

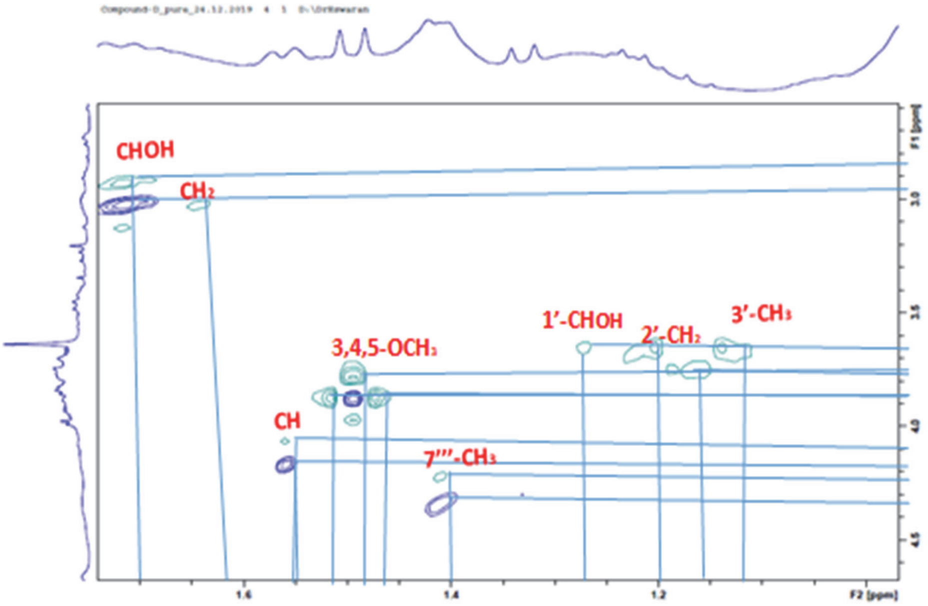

Figure 9. COSY spectrum of Gwal Pahari Acid for δ 0- 1.6 ppm region

Peaks in the region δ 0- 1.6 ppm are shown in (Figure 9). The HMQC spectrum (Figure 10) depicts the correlations between the proton and carbon environment in the molecules. The methoxy signal in this spectrum is again of very high intensity hampering the observation of other signals.

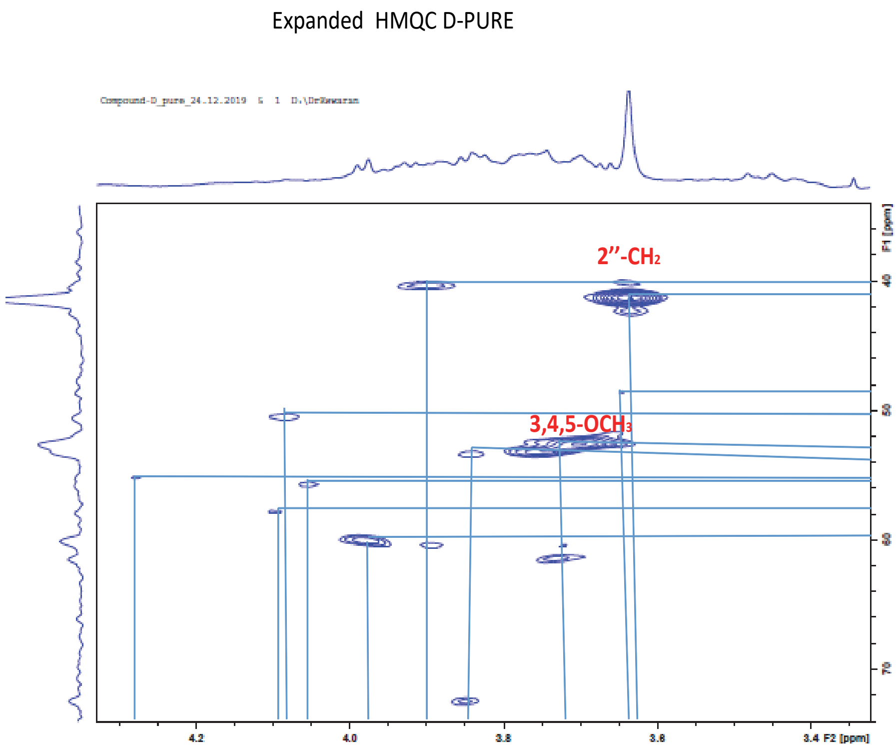

Figure 10. HMQC spectrum of GPA

4.5 Temperature Dependent NMR Spectral Studies

To get a better understanding of the dynamics of the molecule, it was decided to undertake a temperature dependent NMR study. Figure 11 shows the signals observed in the region of δ 0.5- 7.5 ppm.

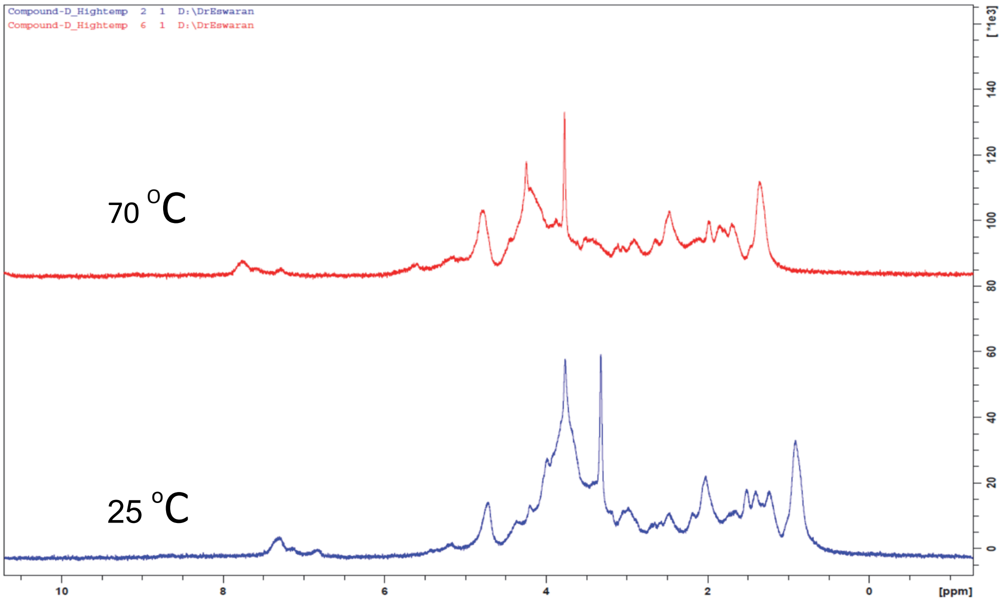

Figure 11. The Temperature dependent ^{1}H NMR spectrum of GPA

4.6 Solid State NMR studies on Gwal Pahari Acid

The solid State NMR spectra were recorded using Bruker 500 MHz instrument and the ^{13}C-CP-MAS-SS-NMR (Helal et al. 2011) at 8 kHz for Gwal Pahari Acid in (Figure 12).

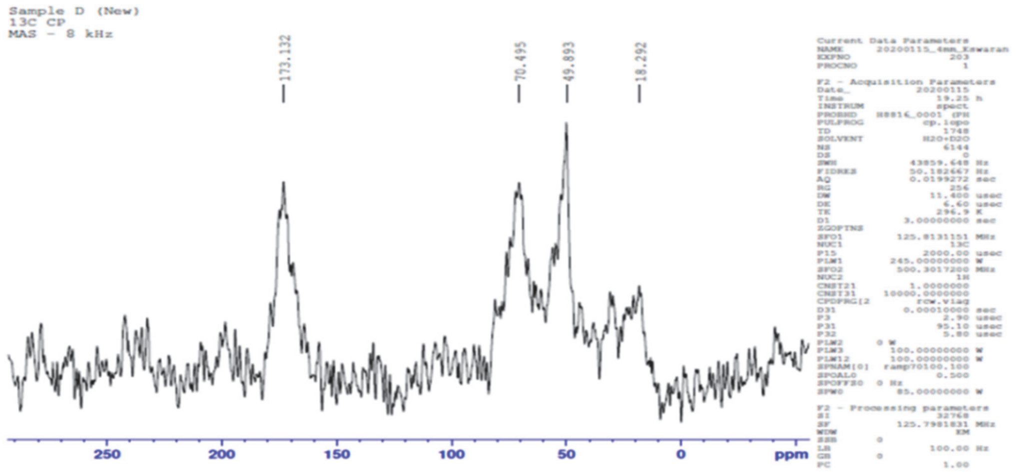

```
Current Data Parameters
NAME       20200115_4mm_Eswaran
EXPNO                   203
PROCNO                    1

F2 - Acquisition Parameters
Date_              20200115
Time                  19.25 h
INSTRUM               spect
PROBHD     H8816_0001 (PH
PULPROG             cp.lopo
TD                     1748
SOLVENT             H2O+D2O
NS                     6144
DS                        0
SWH               43859.648 Hz
FIDRES            50.182667 Hz
AQ                0.0199272 sec
RG                      256
DW                   11.400 usec
DE                     6.60 usec
TE                    296.9 K
D1               3.00000000 sec
ZGOPTNS
SFO1            125.8131151 MHz
NUC1                    13C
P15                 2000.00 usec
PLW1           245.00000000 W
SFO2            500.3017200 MHz
NUC2                     1H
CNST21            1.0000000
CNST31        10000.0000000
CPDPRG[2           rcw.vlag
D31              0.00010000 sec
P3                     2.90 usec
P31                   95.10 usec
P32                    5.80 usec
PLW2       0 W
PLW3           100.00000000 W
PLW12          100.00000000 W
SPNAM[0]    ramp70100.100
SPOAL0                0.500
SPOFFS0    0 Hz
SPW0            85.00000000 W

F2 - Processing parameters
SI                    32768
SF              125.7981831 MHz
WDW                      EM
SSB        0
LB                   100.00 Hz
GB         0
PC                     1.00
```

Figure 12. Solid state NMR spectrum of compound 1a

4.7 Scanning Electron Microscopy (SEM) studies of Gwal Pahari Acid

The SEM pictures generated at 20 µm and 2 µm shown in (Figure 13) was recorded using SEM-Zeiss EVO MA10 in methanolic solution and the size of the 1a is 12.86 nm obtained from zeta size.

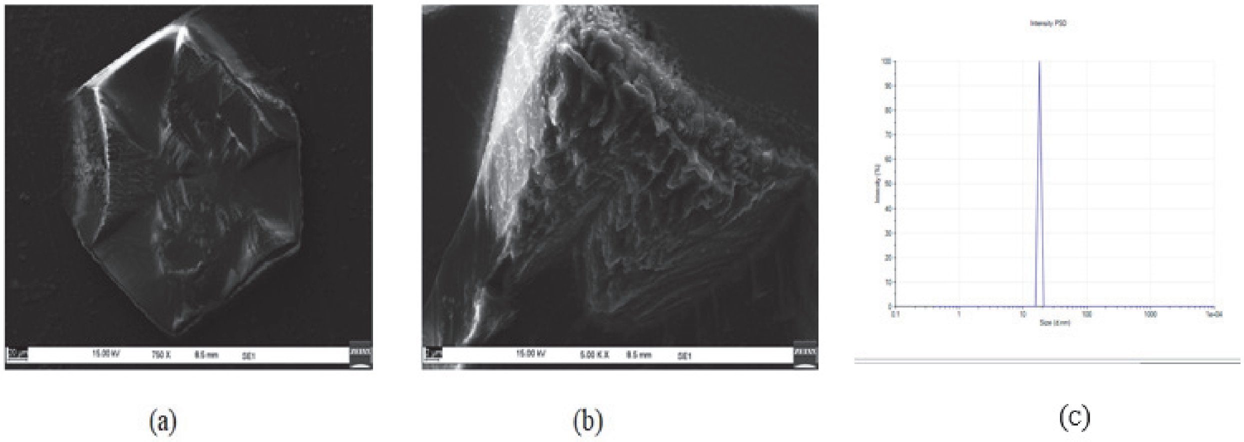

(a) (b) (c)

Figure 13. (a) SEM pictures of Gwal Pahari Acid at (20 µm) (b) SEM picture of Gwal Pahari Acid at (20 µm). (c) Zeta size spectrum of GPA

4.8 Plant Growth Promotory Potential of GPA (Gwal Pahari Acid)

The application of GPA at different concentrations was found to significantly improve the growth of tomato plants (Figures 14).

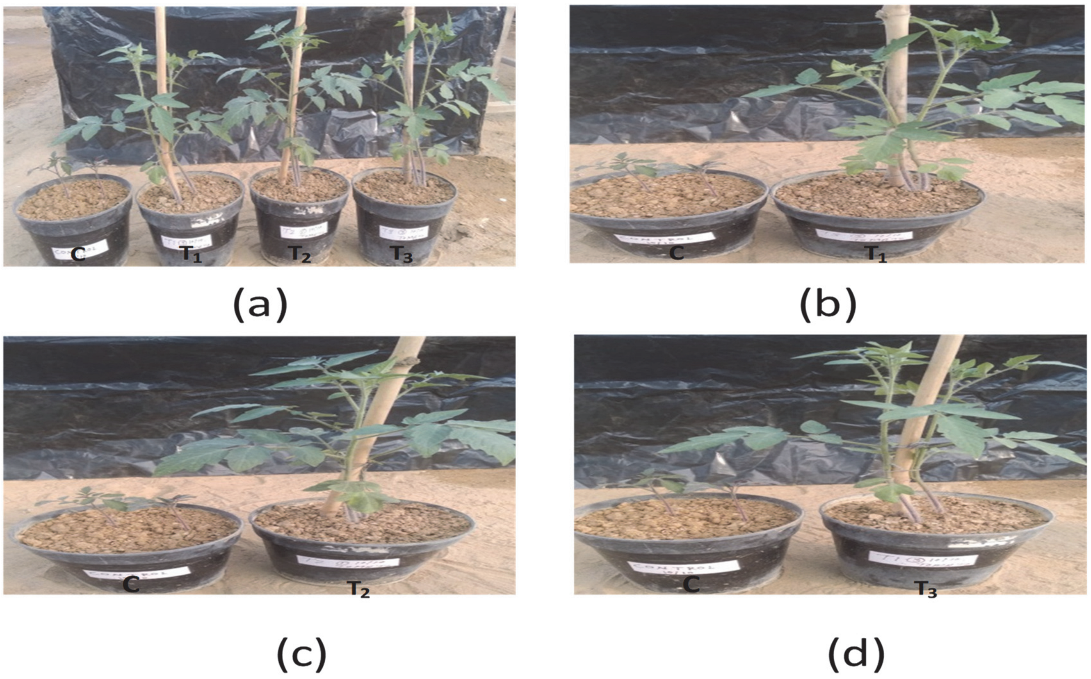

Figure 14. (a) Impact of different conc. of GPA on the growth of tomato plants after 4 weeks, (b) Comparison of plant growth at 100 ppm conc. with untreated control, (c) Comparison of plant growth at 200 ppm conc. with untreated control, (d) Comparison of plant growth at 300 ppm conc. with untreated control. (T_1: 100 ppm, T_2: 200 ppm, T_3: 300 ppm and C: untreated control).

4.9 Studies on Gwal Pahari Acid-Doxorubicin Conjugate

As stated in the introduction, an anti-epileptic drug has been previously bound non-covalently to a humic acid preparation. In this paper we report the preparation of a covalently bonded anti-cancer drug to reduce its side effects. Doxorubicin is the most commonly used anti-cancer drug but it has many side effects. The synthesis of the Gwal Pahari acid- Doxorubicin conjugate was taken up so that the conjugate serves as a slow release anti-cancer drug thus reducing the toxic side effects of Doxorubicin. To be determined or evaluated in clinical studies.

Mass spectral studies of GPA-Doxorubicin Conjugate: Mass spectral studies on the Gwal Pahari Acid-Doxorubicin conjugate have been done using the methanolic solution and the highest obtained peak at m/z 1111.8 is shown in (Figure 15).

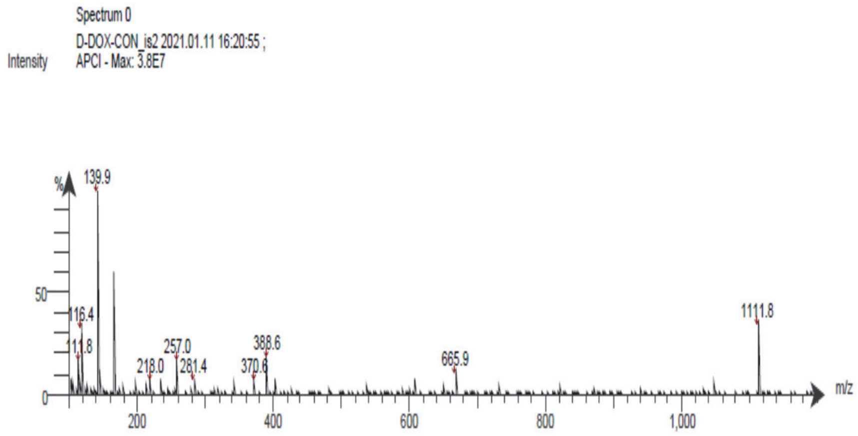

Figure 15. Mass spectrum of GPA-Doxorubicin conjugate

UV- visible spectral studies of GPA- Doxorubicin Conjugate: The UV-visible spectrum of GPA-Doxorubicin conjugate has been recorded in homogeneous methanolic solution which shows absorption at 206, 236, 253, 385, 476, 501 and 534 nm in (Figure 16).

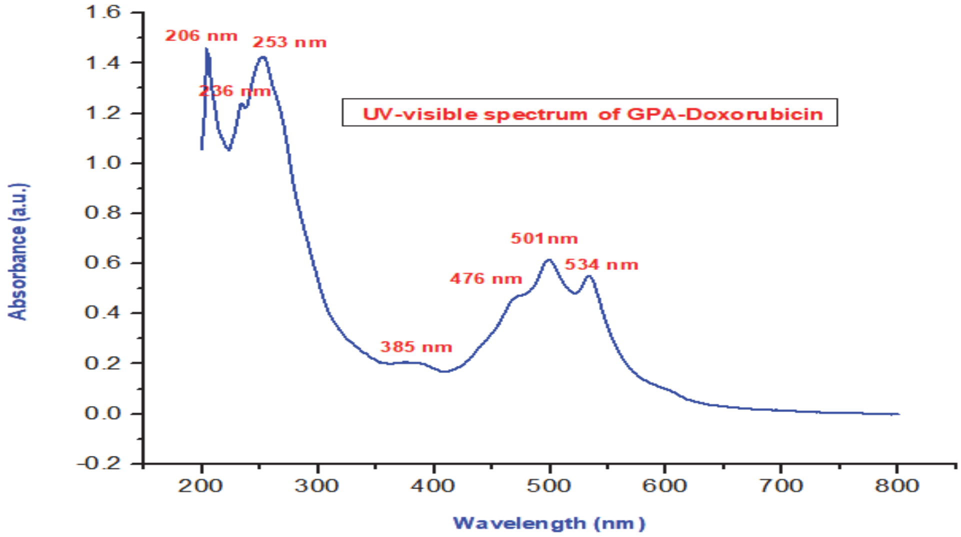

Figure 16. UV-visible spectrum of GPA-Doxorubicin Conjugate

4.10 FT-IR Spectral Studies of GPA-Doxorubicin Conjugate

The FT-IR spectrum of GPA-Doxorubicin conjugate has been recorded in solution phase using methanolic solution and is shown at 462, 623, 829, 923, 1085, 1249, 1378, 1467, 1604, 1743, 2846, 2952 and broad peak at 3419 cm^{-1} in (Figure 17).

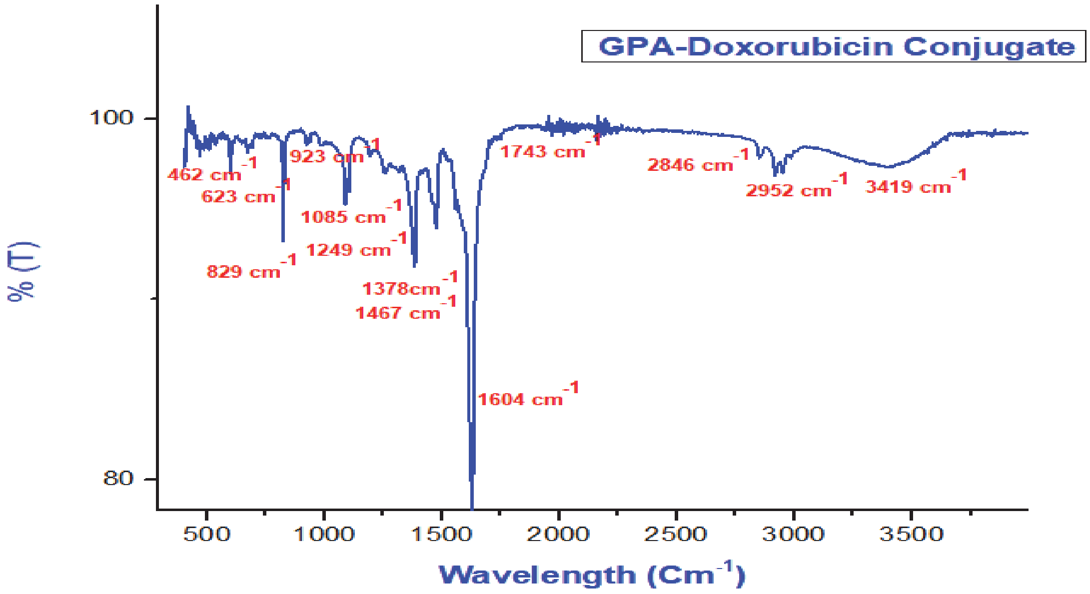

Figure 17. FT-IR spectrum of GPA-Doxorubicin Conjugate

5. Discussion

The new amino acid, a humic acid is water soluble and fluorescent under UV light and shows a positive Ninhydrin test.

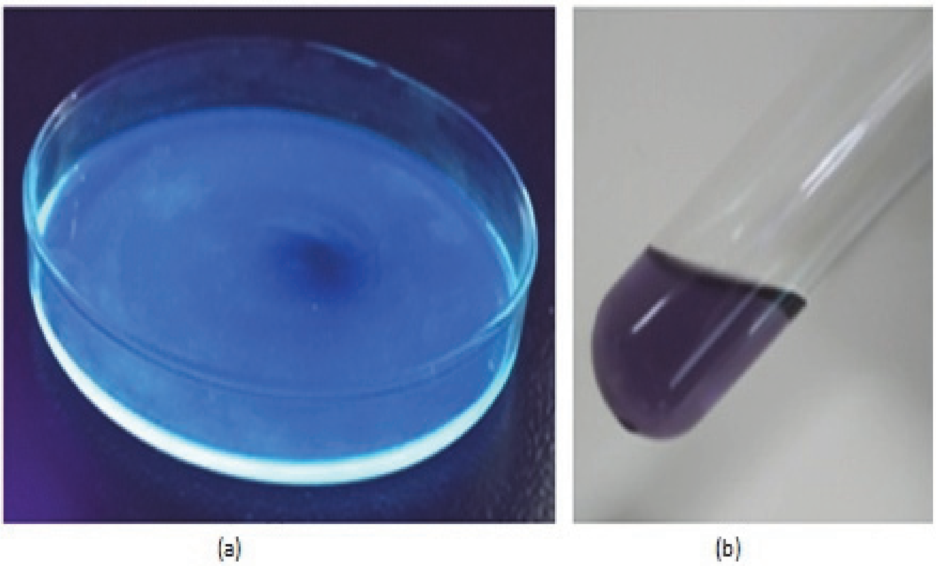

Figure 18. (a) UV- Fluorescence in methanol solution exhibited by Gwal Pahari acid at 366 nm (b) Positive Ninhydrin test shown by Gwal Pahari Acid

The beautiful blue fluorescence (Figure 18 a) shown by the title compound under a UV lamp (366 nm). The positive ninhydrin test of Gwal Pahari Acid is shown in Figure 16b.

5.1 Mass Spectral Studies

The MALDI-MS spectrum of this new compound (Figure 4) showed a peak at m/ z 381.27 and other peaks were observed at m/z 511.37, 503.39, 497.38, 471.39, 437.18, 415.23, 387.32, 359.32, 345.30, 327.27 and 313.26. The GC-MS study of compound 1a showed a peak at m/z 320 (abundance 86.93) and the base peak m/z 319 in (Figure 19).

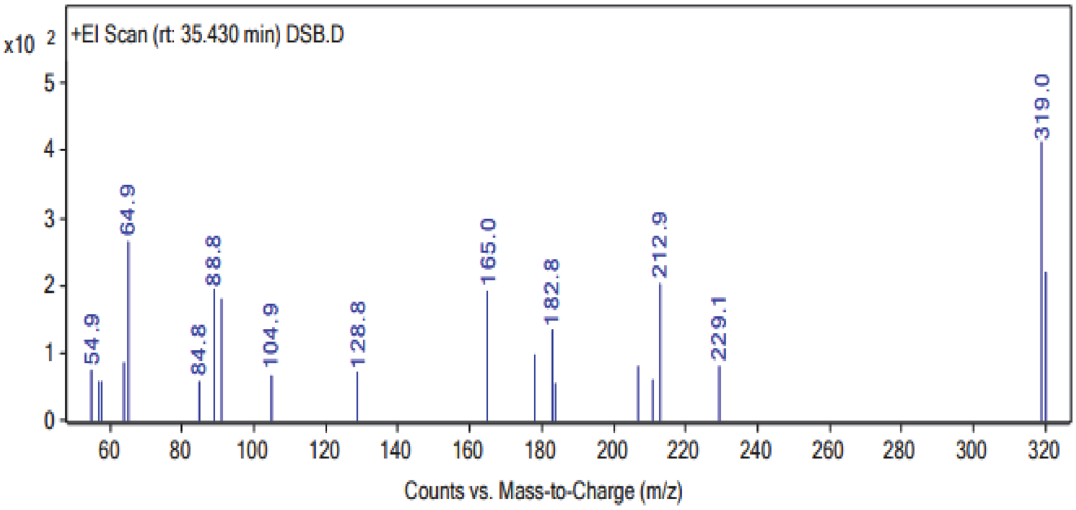

Figure 19. GC-MS spectrum of GPA

Data from these three mass spectral studies helped establish the molecular weight to be 578. Using 'the rule of 13', one arrived at the molecular formula $C_{24}H_{38}O_{14}N_2$.

The molecule consists of three units, viz., Ring A (molecular formula $C_{13}H_{22}NO_8$, observed at m/z 320) and Ring B (molecular formula $C_9H_{12}NO_4$, molecular mass 198) and a two carbon fragment juxtaposed between Ring A and Ring B (molecular formula $C_2H_4O_2$, molecular mass 60, shown by the peak at 380 (381-1H), observed in the MALDI-MS spectrum). Thus, Gwal Pahari Acid has the molecular formula $C_{24}H_{38}N_2O_{15}$, [M^+, and m/z 578.1]. The theoretical molecular weight of the compound is m/z = 578.23 and the error percent thus being 0.02 %.

5.2 UV-Visible Spectral Studies

The UV-visible spectra humic substances were reported and the peaks obtained with slight Shoulder at 205, 320, 375 nm previously (Adekunle et al. 2007). The UV-visible spectrum of Gwal Pahari Acid (Figure 5) showed peaks at 223, 244 and 299 nm, unlike other humic acids, which show absorbance due to phenolics, aromatics, anilines, polyenes, etc. In our case, the spectrum pointed towards absence of such chromophores.

5.3 FT-IR Spectral Studies

The obtained peaks at 3461 cm^{-1} (very broad peak due to hydrogen bonded hydroxyl groups and (N–H), 2999 (aliphatic C–H groups), 1692 (C=O group), 1423 (aliphatic C–H groups), 961 (C–C of alcohol, ether, ester, polysaccharide groups and O–H of alcohol), 576 cm^{-1} (N-C-C=O) of carboxyl) and other peaks 2115 and 2422 cm^{-1} were also present [*loc.cit.*].

5.4 Optical Activity

Based on proposed structure and optical properties (Kwon, D. et. al. 2018) there are 13 chiral centers and according to (2^n) rule, where n is equal to the number of chiral centers, the number of optical isomers possible is 8192. The new compound showed the α_D of -4.40.

5.5 ^{1}H-NMR Spectral Studies

As we undertook NMR spectral studies on Gwal Pahari Acid it was clear that this is not going to be a trivial exercise and hence was undertaken in three different research institutes in India**.** No signal was observed in aromatic region at all. The strong signal at δ 3.33 is assigned to the methoxy group and dominated the spectrum. In the region a broad peak was observed at δ 0.93 ppm, showing the presence of methyl group. Since the ^{1}H-NMR spectrum was recorded in D_2O, no signals were expected to be observed due to groups containing rapidly exchangeable hydrogens e. g. protons of the -COOH and –OH groups. Ring A is relatively more flexible and is capable of pseudorotation and showed multiple signals, with fractional intensity, which supports its flexible nature. Ring B, on the other hand, constitutes the more rigid bicyclo (2. 2. 1) hexane system. In between, the Ring A and ring B, is the highly sterically hindered tetrahedral carbon atom, with its somewhat restricted rotation possibilities. It is suggested that the conformations that can be occupied by Ring A and the attached tetrahedral carbon are bound to influence Ring B. The assignments of the different protons in the new compound are shown in Table 1.

Table 1. Assignments of the protons in the ^{1}H-NMR spectrum of GPA

Position of Ring	Position of Proton	Chemical Shift in proton NMR	Assignment
Ring A	C-3	3.33 (s)	3-O<u>CH₃</u>
Ring A	C-4	3.33(s)	4--O<u>CH₃</u>
Ring A	C-5	3.33(s)	5-O<u>CH₃</u>
Ring A	C-2	3.20-3.28 (m)	2-C<u>H</u>
Ring A	C-3	3.38-3.42 (m)	<u>CH</u>
Ring A	C-1'	3.53-3.58 (m)	<u>CH</u>
Ring A	C-2'	1.51(q)	<u>CH₂</u>
Ring A	C-3'	0.93 (t)	<u>CH₃</u>
Ring A and Ring B	C-1, 2, 1''', 2'''		COOH

Between ring A and B	C-1’’		
Between ring A and B	C-2’’	3.46.3.53 (m)	-CH_2
Ring B	C-1’’’		
Ring B	C-2’’’	2.55-2.58(d)	CH
Ring B	C-3’’’	2.25 (dd)	CH
Ring B	C-4’’’	2.2 (dd)	CH
Ring B	C-5’’’	2.48(d)	CH
Ring B	C-6’’’	2.11 (q)	6’’’-CH
Ring B	C-7’’’	1.2-1.4 (m)	-CH_3 Bridge
Ring B			

The use of MATLAB-GUI interface using ^3JH coupling in simple five membered rings has been proposed[23] However, our system is much more complex and would require further detailed mathematical analysis to understand the role of pseudo rotation, if any, in our system.

The ^{13}C NMR spectrum also put up surprises as only the signal for the methoxy group alone could be observed at 49.0367 ppm.

5.5 2D-NMR spectral studies of Gwal Pahari Acid:

In Ring A there are three methoxy groups observed at δ 3.6-3.8 as shown in Table 2 (earlier observed at δ 3.33, attributed to nine protons at position 3, 4, 5. The highly shielded signal at δ 0.93 is assigned and shown in Table 2.

The HSQC spectrum clearly provides evidence of correlation of methoxy peak at δ 3.33 in ^1H NMR and the different carbons and hydrogen in GPA. The presence of CH_3, CH_2, CHOH, CH groups and the methoxy peaks present at position 3, 4, 5. Combining ^1H-NMR and 2D-NMR using HSQC spectrum showing the correlations and for better understanding of the molecular environment. The assignments based on 1-D and 2-D NMR is shown in Table 2.

Table 2. Correlations determined using 2D-NMR data

^{13}C-NMR chemical shift values in ppm	Carbon	COSY (ppm)	HSQC (ppm)
52.5	-O-C-3	1.1-1.3(H-1’, 2’, 3’) -3.6-3.8 (H- 3,4,5)	1.51-23.5 (C-2’)
49.85	-O-C-4	1.41-1.52 (H-??)- 3.68-3.89 (	1.95-35 (C-4’’’)
53.5	-O-C-5	1.4 (CH_3-7’’’)	2.05-28 (C-6’’’)
37.5	C-2	1.45-1.52 (H-2)-3.6-3.8(3,4,5- OCH_3)	2.1-26 (C-3’’’)
57.2	C-3	1.32 -4.2	2.55-51 (C-2’’’)
59.5	C-1’	1.61(H-2’)-1.95(H-6’’’)	3.1-45(C-3’’’)
23.5	C-2’	1.70-1.85,1.95	3.20-37.5 (C-2)
18.2	C-3’		3.6- 48.89, 52.5,53.5 (C-3,4,5 OCH_3)
173.17	C-1		3.85-59.5 (C-1’)
	C- 2		
	C-1’’’		

	C-2’’’		
70.49	C-1’’		3.98-62.5 (C-2’’)
62.5	C-2”		
67.5	C-1’”		
51.0	C-2’’’		
26.0	C-3’’’		
35.0	C-4’’’		
45.0	C-5’’’		
28.0	C-6’’’		
58.0	C-7’’’’		
27.5	Bridge Head Quat. Carbon		

The signal at δ1.1 and 1.3 (H-1’, 2’, 3’) correlates with 52.5 ppm and also correlates with 3.6-3.8 (H- 3,4,5) .

5.6 Temperature Dependent NMR spectral Studies

The NMR spectrum of GPA showing at 25^0 C (in blue) are shifted towards higher delta values at 70^0 C confirming the dynamic nature of parts of the molecule, which is also confirmed by the analysis of other NMR spectrum.

5.7 Solid State NMR studies on Gwal Pahari Acid

FT-IR spectrum and the alkali solubility of compound 1a indicated the presence of the carboxylic acid, but our ^{1}H-NMR studies could not provide clinching evidence for the presence of carboxylic acid group (s). Hence we undertook solid state NMR studies.

This study provided evidence for the presence of carboxylic acid at 173.132, CH_2OH at 70.495, methoxy signal at 49.893 and the methyl group peak at 18.292. Solid state NMR studies thus confirmed the new compound being a carboxylic acid (Table 3).

Table 3. Assignments based on Solid state NMR analysis of GPA

Peaks of Carbon δ (ppm)	Position of Carbon	Groups
18.292	C-3’	$-CH_3$
49.893	OCH_3-3,4,5	$-OCH_3$
70.495	C-2”	$-CH_2OH$
173.132	COOH- 1, 2, 1’”, 2’”	-COOH

5.8 Scanning Electron Microscopy (SEM) studies of Gwal Pahari Acid:

Previous SEM studies (Yang et al. 2020) on similar compounds also have established the crystalline property of such compounds and their crystal morphology are showing special granular surface.

5.9 Chemical Structures of GPA and GPA-Doxorubicin Adduct

Based on above data the chemical structure of GPA is shown in (Figure 20). Its 3D structure based on the Chem Draw software.

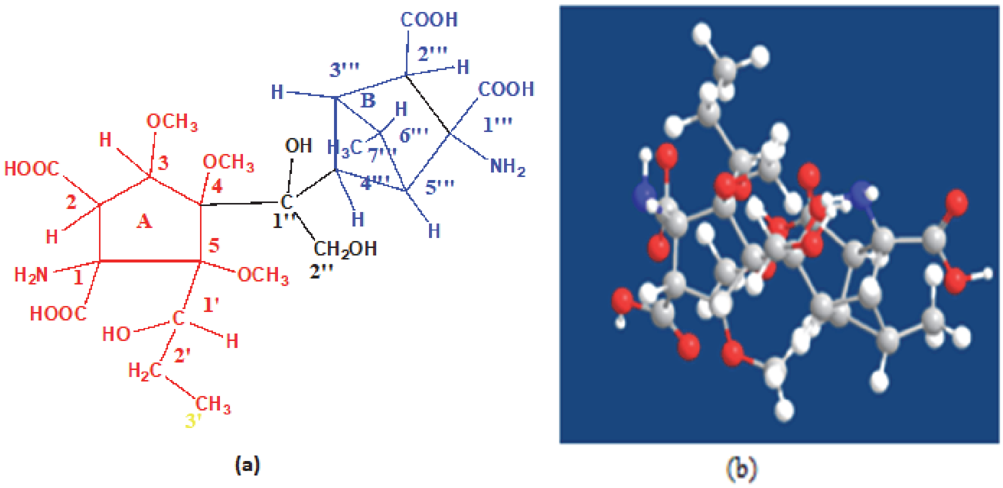

Figure 20. (a) The proposed structure of "Gwal Pahari Acid" (b) 3D structure of Gwal Pahari acid

Ring A of the structure is a relatively flexible substituted cyclo pentane ring. Ring A is flexible and capable of showing pseudo rotation which makes NMR measurements very difficult. Ring B on the other hand is a cyclo pentane ring system, which is a methylene bridged which makes it conformationally rigid. Ring A and Ring B are connected to each other through a tetra-substituted sp^3 carbon atom. The systematic name of the title compound, Gwal Pahari Acid is 2-Amino-2, 3 dicarboxy-1-(1-propan-1-ol-yl)-5-(2-amino-2, 3-dicarboxy-1, 4, 5-trimethoxy cyclopentyl-1-(hydroxyl-1-hydroxymethyl)-6-methylbicyclo [2.1.1] hexane.

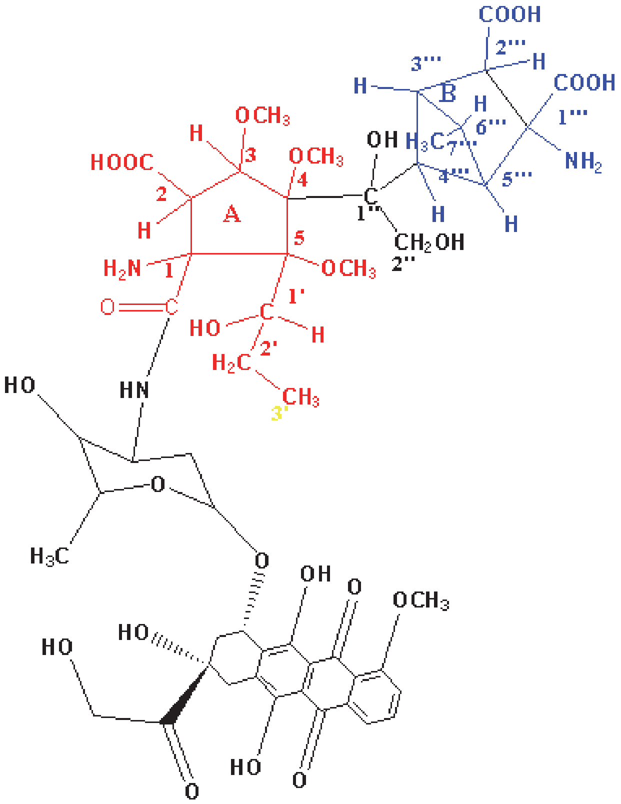

Scheme 2. The proposed structure of GPA-Doxorubicin conjugate

Based on the spectroscopic data the structure of a mono adduct of GPA is shown in Scheme 2.

5.10 Plant Growth Promotory Potential of GPA (Gwal Pahari Acid)

Although treatment with GPA also showed significant increase at 100 ppm and 200 ppm when compared with untreated control, however the highest improvement was recorded at 300 ppm (Figure 21). At higher conc. 400 ppm and 500 ppm of GPA, the plant growth was significantly reduced and the plants gave a burning appearance, therefore GPA at 400 ppm conc. and above seems detrimental to plant growth (loc. cit.). There were no significant difference observed among the treatments T2 (200 ppm) and T3 (300 ppm) in terms of improvement of plant growth parameters studied except root length, however differences observed between T1 (100 ppm) and T3 (300 ppm) were significant.

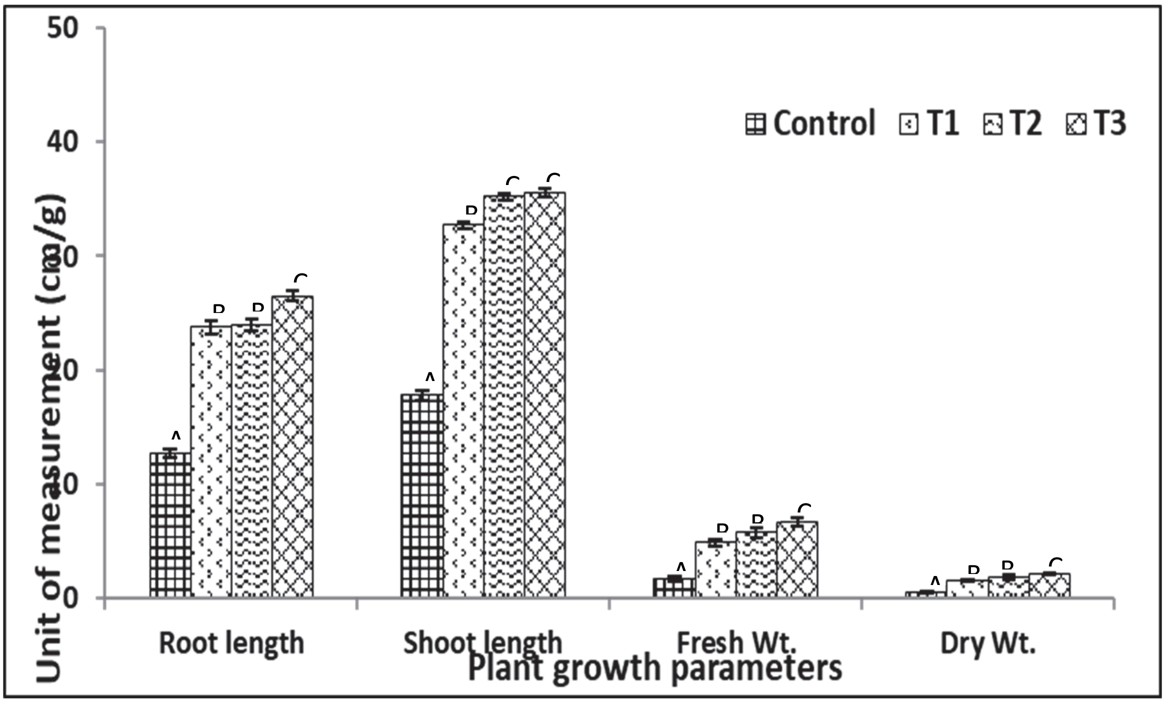

Figure 21. Impact of GPA on plant growth parameters at different conc. (T_1: 100 ppm, T_2: 200 ppm, T_3: 300 ppm and Control: untreated). Different letters indicate significant difference ($p \leq 0.05$) between treatments

However, GPA at conc. 300 ppm showed highest improvement in plant growth (Figure 14 c). There was 108% increase observed in the root length while shoot length was increased by nearly 100% in tomato plants treated with 300 ppm GPA as compared to control. Similarly, a significant increase in the fresh wt. (>290%) as well as dry wt. (>290%) was also observed in the plants treated with GPA 300 ppm.

5.11 Ion Leakage Assay Studies Using Arabidopsis Thaliana as Model Plant System

We took 1 g of plant tissue from both the treated as well as the control sample in 10 ml non-ionized Millipore distilled water and kept it for 3 hours under vigorous tumbling condition. Then the water was decanted into a sterile glass container and comparatively measured the released ions through conduction meter (Figure 22).

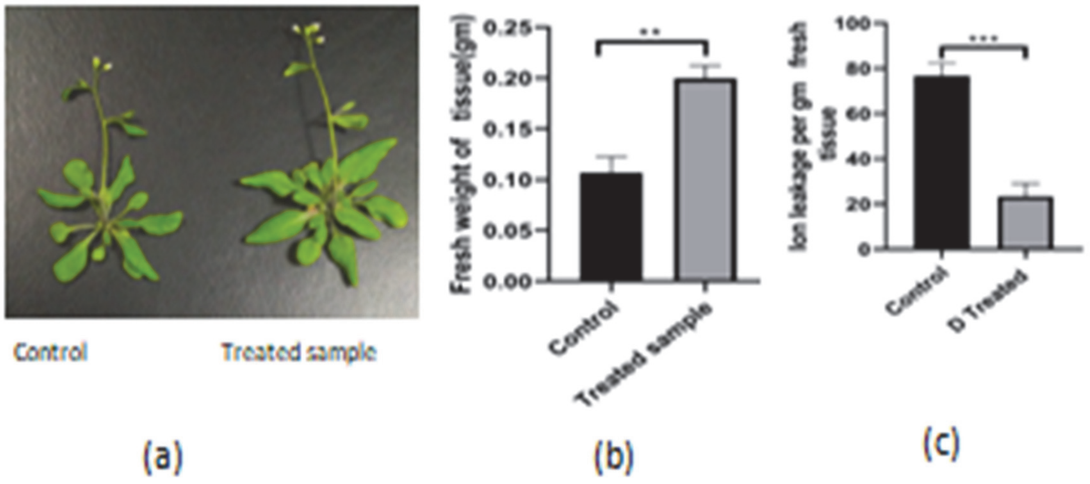

Figure 22. (a) Picture of treated and control in growth (b) Fresh weight of treated and control (c) Ion leakage assay results in treated and untreated *Arabidopsis thaliana*

Gwal Pahari Acid helps the plant to reduce the ion leakage and thus helps to the strengthening cell wall stability [loc. cit].

5.12 Studies on Gwal Pahari Acid-Doxorubicin Conjugate:

5.13 Mass spectral studies of GPA-Doxorubicin Conjugate

The molecular Ion peak of Gwal Pahari Acid is 578.1 and the molecular formula being $C_{24}H_{38}O_{14}N_2$ and after losing a hydrogen the peak was obtained at m/z 577.1. Conjugated with Doxorubicin ($C_{27}H_{29}NO_{11}$, 543.52) with Gwal Pahari acid (578.1) yields the peak at m/ z 1111.8 (i. e., 578.1- 17.00 (OH) = 561.1; + 542.5 + 39.09 (K) = m /z 1142.69– 31.03 (OCH_3) = m/z 1111.66. Observed m/z; 1111.80, Error percentage is 0.01 %; calculated based on obtained peak.

5.14 UV- Visible Spectral Studies of GPA- Doxorubicin Conjugate:

In these studies we observed peaks at 206, 236 and 253 nm and at 385, 476, 501 and 534 nm showing the presence of both Gwal Pahari Acid and Doxorubicin, though somewhat blue shifted due to conjugation (Bandak et al. 1999).

5.15 FT-IR Spectral Studies of GPA- Doxorubicin Conjugate:

The FT-IR spectrum of Gwal Pahari Acid -Doxorubicin conjugate showed peaks at 923 cm^{-1} (C-O-bending), 1085 cm^{-1} , 1249 cm^{-1}(C-O stretching), 1378 cm^{-1} (O-H bending), 1467 cm^{-1} (Ring C-H bending), 1604 cm^{-1} (C-H bending), 1743 cm^{-1} (C=O), 2846 cm^{-1} (C-H stretching), 2952 cm^{-1} (C-H stretching) and 3419 cm^{-1} (O-H Stretching) which shows the presence of Doxorubicin and confirms the conjugation of Doxorubicin with Gwal Pahari Acid (Gautam et al. 2021).

6. Conclusion

A new Humic acid has been isolated from the soil of Gwal Pahari, Gurgaon, Haryana, India. It shows a positive Ninhydrin test and contains both partly rigid and dynamic five-membered ring systems, one of which is capable of exhibiting pseudorotation. Spectroscopic studies like FT-IR, UV-visible spectroscopy, and mass spectrometry helped in putting up the proposed structure. However, detailed NMR studies [^{1}H- NMR; 2D-NMR (COSY, HSQC, HMBC; CP-MAS-SS-NMR)], though challenging, and helped arriving at the structure of the new compound.

Based on ion leakage studies, the new compound has been shown to protect the model plant *Arabidopsis thaliana.* The greenhouse studies showed that Gwal Pahari Acid (GPA) has significant potential to improve plant growth and may be used as an adjuvant in combination with other PGPRs and/or bio-fertilizers in organic agriculture.

However, further studies are required to determine its impact on various economically important crops across various agro-climatic conditions.

Studies like the present one could help grow better vegetables, quality fruits (peas, potatoes, tomatoes, pomegranates, mangoes) cereals and pulses. Humic acids present in soil, lignite, city solid waste and compost can also lead to similar compounds, which lead to increased agricultural output. These could lead to reduction in the uses of inorganic substances in agriculture and highlight the natural organic plant nutrients present in soil leading to a positive impact on the environment and climate change. Such humic acids also have a role in material science [(e. g., Dye Sensitized Solar cells (DSSC)], which could contribute to the energy sector of economy.

Conflict of interest

The authors declare no conflict of interest.

Author Contribution

SVE conceptualized and planned the work and drafted the manuscript; SKT did the synthesis, characterization and helped in manuscript preparation; KG performed the ion leakage experiments; AK carried out plant growth work on tomato and greenhouse experiments and SB conceptualized and supervised the plant work on *Arabidopsis thaliana*.

Acknowledgements

Authors thank Dr. Alok Adholeya, Executive Director, Teri Deakin Nano Biotechnology Research Center (TDNBC), TERI Gram, Gwal Pahari, Gurgaon Faridabad Expressway, Gurugram, and Haryana 122002 for facilities. Authors thank the Executive Director, Regional Centre for Biotechnology (RCB) Faridabad, Haryana, India and for research facilities. Authors thank CMD, NSIC, Mr. M. A. Khan, Mr. O. P. Singh, and Mr. Sanjay Sarif, NSIC Technical Center, Okhla Phase III, New Delhi for providing facilities. We thank Dr. Vipin Agarwal (Assosiate Professor), Dr. Krishnarao (Scientific Officer), Tata Institute of Fundamental Research, Hyderabad (TIFR-H) for NMR work. We thank Dr. Dinesh Mahajan (THSTI, Faridabad) for his unconditional support. We thank Ms. Priyanka Gupta, Ms. Deep Rajni and Mr. Chandrakant Tripathi for Zeta size and SEM studies. Authors thank Mr. Puran Chandra Prusty for help in experimental work in the extraction of Gwal Pahari acid and Mr. Satendra Kumar for support in plant work.

†c/o Incubation Center, Industrial Estate, NSIC Technical Services Centre, Okhla Phase III, New Delhi-110020.

References

Abakumov, E., Lodygin, E., & Tomashunas, V. (2015). ^{13}C NMR and ESR Characterization of Humic Substances Isolated from Soils of Two Siberian Arctic Islands. *International Journal of Ecology, 1,* 1-7. https://doi.org/10.1155/2015/390591, 2015

Adekunle, I. M., Arowolo, T. A., Ndahi, N. P., Bello, B., David A., & Owolabi, D. A. (2007). Chemical Characteristics of humic acids in relation to the Lead, Copper, and Cadmium levels in contaminated soil from South West Nigeria; *Annals of Environmental Science*, *1,* 23-34. http://hdl.handle.net/2047/d10006084, 2007.

Al-Faiyz, Y. S. S. (2017). CP-MAS ^{13}C-NMR characterization of humic acids from composted agricultural Saudi waste, *Arabian J. Chem*., *10*, S839-S853. https://doi.org/10.1016/j.arabjc.2012.12.018

Bandak, S., Ramu, A., Barenholz, Y., & Gabizon, A. (1999). Reduced UV-induced degradation of Doxorubicin encapsulated in polyethyleneglycol-coated liposomes. *Pharm Res.*, *16*(6), 841-6. https://doi.org/10.1023/a:1018869818282, 1999.

Beckely, V. A. (1921). The preparation and fractionalization of humic acid. *J. Agric. Sci*., *11,* 66-68. https://doi.org/10.1017/S0021859600003518

de Melo B. A. G., Motta, F. L., & Santana, M. H. A. (2016). Humic Acids: Structural Properties and Multiple Functionalities for Novel Technological Developments. *Materials Science & Engineering C*, C 62, 967-974. https://doi.org/10.1016/j.msec.2015.12.001

De Nobili, M., Bragato, G., Alcaniz, J. M., Puigbo, A., & Comellas, L. (1990). Characterization of electrophoretic fractions of humic substances with different electrofocusing behavior. *Soil Sci*., *150*, 763-770.

Ekin, Z. (2019). Integrated Use of Humic Acid and Plant Growth Promoting Rhizobacteria to Ensure Higher Potato Productivity in Sustainable Agriculture, *Sustainability*, *11,* 3417. https://doi.org/10.3390/su11123417

Eladia, M., Peña-Méndez, Havel, J., & Patočka J. (2005). Humic substances-compounds of still unknown structure: applications in agriculture, industry, environment, and biomedicine, *Journal of Applied biomedicine*, 3, 13-

24. https://doi.org/10.32725/jab.2005.002

El-Metwally, M., Selim., Ahmad A. T., Mosa, A. A., & EL-Agamy, M. A. (2014). Chemical Composition of Humic Substances Extracted from Salt Affected Egyptian Soils. *Life Sci. J.*, *11*(9), 197-206. ISSN:1097-8135, 2014.

Fasurova, N., & Pospisiova, L. (2010). Characterization of soil humic of soil by Ultraviolet-visible and synchronous fluorescence spectroscopy. *Journal of Central European Agriculture*, 11(3), 351-357.

Gajdosová D., Pokorná L., Láska S., Prosek, P., & Havel, J. (2001). Are there humic acids in Antarctica? In Ghabbour E.A., Humic Substances: Structures, Models and Functions, (Eds.Ghabbour,E. A. &Davis, G.)Xiii+387 pp. Cambridge: *Royal Society of Chemistry,* ISBN 0 85404 811 1, RSC, Cambridge*,* 121-131. https://doi.org/10.1017/S0021859602252259

Gajdošová, D., Novotná, K., Prošek, P. & Havel, J. (2003). Separation and characterization of humic acids from Antarctica by capillary electrophoresis and matrix-assisted laser desorption ionization time-of-flight mass spectrometry: Inclusion complexes of humic acids with cyclodextrin, *Journal of Chromatography A*, 1014, 1-2, 117-127. https://doi.org/10.1016/S0021-9673(03)01040-9, 2003.

Gautam, R. K., Navaratna, D., Muthukumaran, S., Singh, A., Islamuddin, I., & More, N. (2021). Humic Substances: Its Toxicology, Chemistry and Biology Associated with Soil, Plants and Environment. In (Ed.) in: Humic Substances, Ed. Abdelhadi, *Intechopen*, https://doi.org/10.5772/intechopen.98518, 2021.

Giovanelaa, M., Crespoa, J. S., Antunesa, M., Adamattia, D. S., Fernandesa, A. N., Barisonb, A., … Sierrad, M. M. D. (2010). Chemical and spectroscopic characterization of humic acids extracted from the bottom sediments of a Brazilian subtropical microbasin, *Journal of Molecular Structure, Elsevier, 981*(1-3), 111-119. https://doi.org/10.1016/j.molstruc.2010.07.038, 2010.

Hatsugai, N., & Katagiri, F. (2018). Quantification of Plant Cell Death by Electrolyte Leakage Assay. *Bio-protocol*, *8*(5), e2758. https://doi.org/10.21769/BioProtoc.2758, 2018.

Helal, A. A., Murad, G. A., & Helal, A. A. (2011). Characterization of different humic materials by various analytical techniques, Characterization of different humic materials by various analytical techniques. *Arabian Journal of Chemistry*, *4*(1), 51-54. https://doi.org/10.1016/j.arabjc.2010.06.018, 2011.

Hendrickx, P. M. S., & Martins, J. C. (2008). A user-friendly Matlab program and GUI for the pseudorotation analysis of saturated five-membered ring systems based on scalar coupling constants. *Chemistry Central Journal*, *2*(20),1-7. https://doi.org/10.1186/1752-153X-2-20, 2008.

Kwon, D., Sovers, M. J., Grassian, V. H., Kleiber, P. D., & Young, M. A. (2018). Optical Properties of Humic Material Standards: Solution Phase and Aerosol Measurements, *ACS Earth and Space Chemistry, 2*(11), 11021111. https://doi.org/10.1021/acsearthspacechem.8b00097, 2018.

Mirza, M. A., Agarwal, S. P., Rahman, M. A., Rauf, A., Ahmad, N., Alam, A., & Iqbal, Z. (2011). Role of humic acid on oral drug delivery of an antiepileptic drug, Drug *Dev. Ind. Pharm.*, 37, 310–319. https://doi.org/10.3109/03639045.2010.512011, 2011.

Piccolo, A. (2002). The supramolecular structure of humic substances: A novel understanding of humus chemistry and implications in soil science; *Advances in Agronomy, 75,* 57-134. https://doi.org/10.1016/S0065-2113(02)75003-7, 2002.

Shinozuka, T., Shibata, M., & Yamaguchi, T. (2004). Molecular Weight Characterization of Humic Substances by MALDI-TOF-MS. *J. of mass. Spectrom. Soc. Jpn.*, 52(1), 29-32. https://doi.org/10.5702/massspec.52.29, 2004.

Stenson, A. C., Landing, W. M., Marshall, A., G., & Cooper, W. T. (2002). Ionization and Fragmentation of Humic Substances in Electrospray Ionization Fourier Transform-Ion Cyclotron Resonance Mass Spectrometry, *Anal. Chem., 74,* 4397-4409.https://doi.org/10.1021/ac020019f, 2002.

Subramanian, P., Mageswari, A., Kim, K., Lee, Y., & Sa, T. (2015). Psychrotolerant endophytic Pseudomonas sp. strains OB155 and OS261 induced chilling resistance in tomato plants (*Solanum lycopersicum Mill.*) by activation of their antioxidant capacity. *Mol. Plant-Microbe Interact*., *28,* 1073–1081. https://doi.org/10.1094/MPMI-01-15-0021-R, 2015

Swidsinski, A., Dörffel ,Y., Loening-Baucke ,V., ChristophGille , C., Reißhauer, A., O., Krüger, M. Neuhaus , J., & Schrödl, W. J. (2017). Impact of humic acids on the colonic microbiome in healthy volunteers. *World, J Gastroenterology*, *7*, 23(5), 885-890. https://doi.org/10.3748/wjg.v23.i5.885, 2017

Tan, K. H. (1985). Scanning Electron Microscopy of Humic Matter as Influenced by Methods of Preparation. *Soil*

Sci. Soc. Am. J., *49*, 1185-1191.https://doi.org/10.2136/sssaj1985.03615995004900050023x, 1985.

Tatzber, M., Spiegel, H., Katzlberger, C., Haberhauer, G., Mentler, A., & Gerzabek, M. H. (2007). FT-IR spectroscopic characterization of humic acids and humin fractions obtained by advanced NaOH, $Na_4P_2O_7$, and Na_2CO_3 extraction procedures, *J. Plant Nutr. Soil Sci., 170,* 522–529. https://doi.org/10.1002/jpln.200622082, 2007.

Thurman, E. M., & Malcolm, R. L. (1981). Preparative isolation of aquatic humic substances. *Environ. Sci. Technol, 15,* 463-466. https://doi.org/10.1021/es00086a012, 1981.

Vekariya, R. L., Sonigara, K., K., Fadadu, K. B., Vaghasiya, J. V., & Soni, S. S. (2016). Humic Acid as a Sensitizer in Highly Stable Dye Solar Cells: Energy from an Abundant Natural Polymer Soil Component, *ACS Omega*, 1, 14–18. https://doi.org/10.1021/acsomega.6b00010, 2016.

Yang, F., Zhang, S., Fu, Q., & Antonietti, M. (2020). Conjugation of artificial humic acids with inorganic soil matter to restore land for improved conservation of water and nutrients, *Land Degrad Dev., 31,* 884–893. https://doi.org/10.1002/ldr.3486, 2020.

Copyrights